Desalination and Water Treatment
www.deswater.com

doi: 10.5004/dwt.2017.20378

67 (2017) 215–222
March

Cadmium ions removal from acid aqueous water by chicken eggshells

Ting Zhang[a], Guining Lu[a,b,c,*], Zhihong Tu[a], Lu Qu[a], Chuling Guo[a,b], Zhi Dang[a,b]

[a]*School of Environment and Energy, South China University of Technology, Guangzhou 510006, China, Tel. +86-20-39380512; Fax: +86-20-39380508; emails: GNLu@foxmail.com (G. Lu), 1533433925@qq.com (T. Zhang), 543897490@qq.com (Z. Tu), 596674584@qq.com (L. Qu), clguo@scut.edu.cn (C. Guo), chzdang@hotmail.com (Z. Dang)*
[b]*The Key Laboratory of Pollution Control and Ecosystem Restoration in Industry Clusters, Ministry of Education, Guangzhou 510006, China*
[c]*Guangdong Provincial Engineering and Technology Research Center for Environmental Risk Prevention and Emergency Disposal, Guangzhou 510006, China*

Received 31 July 2016; Accepted 19 November 2016

ABSTRACT

Chicken eggshells (ES) were used to remove cadmium ions from acid aqueous water. The presence of (Ca, Cd)CO_3 crystals has been corroborated by scanning electron microscope with element mapping. Combining with the decreasing pH values as Cd^{2+} concentration increases, the removal process was dominated by precipitation and cation exchange. The cation exchange occurred at low concentrations, and precipitation dominated the removal mechanism at high concentrations. In binary metals competitive experiment of Cd^{2+}–Cu^{2+} and Cd^{2+}–Pb^{2+}, at low concentrations of Cu^{2+} and Pb^{2+}, the removal capacity of Cd^{2+} did not decrease obviously; while at high concentrations of Cu^{2+} and Pb^{2+}, the Cd^{2+} ions were at a competitive disadvantage. The Langmuir model fitted equilibrium data better than Freundlich model. The certified endothermic and favorable sorption had maximum uptake of 2.40 mg g^{-1} for Cd^{2+} on ES at 298 K. The adsorption process better followed pseudo-second-order kinetics, and the activation energy was 23.67 kJ mol^{-1}; both showed the chemical sorption being the rate-controlling step. The results indicated that the removal efficiency of cadmium ions had reached above 90% on ES of diameter 0.45–1.0 mm in solution of pH 4.5 and 7.6 mg L^{-1} Cd^{2+}.

Keywords: Cadmium; Eggshell; Calcite; Cation exchange; Precipitation; Langmuir isotherm; Pseudo-second-order kinetics

1. Introduction

Heavy metal pollution is a serious environmental and health hazard. Cadmium, in particular, exhibits significant hazard in ecosystem especially in human health, because it accumulates easily through food chain [1]. Although several treatments such as chemical precipitation, ion exchange and solvent extraction have been used for cadmium removal, biomaterial adsorption possesses particular strengths because it is eco-friendly, abundant and low-cost [2,3]. The environmental applications of biomaterial can reduce the quantity of hazards caused by other materials effectively and have distinct advantages over conventional technologies, since the process does not produce chemical sludge, less secondary pollution [4]. Previous researchers have studied biological waste materials, such as green algae and rice hulls [5], crab shell [6], grape bagasse [7], wheat residue [8] and so on. However, the feasibility of utilizing chicken eggshells to remove cadmium ions in acid water is seldom reported.

The combination of low pH and high metal concentrations has a significant negative impact on plant condition and epiphytes. However, significantly more metals were removed in the pH-adjusted treatment. Calcium carbonate, which is the major component of ES (up to 89.5% $CaCO_3$) [9], could perform as a potential contributor to low acidity and act as a worthy material for immobilizing heavy metals in water and soil as well [10].

* Corresponding author.

According to the National Bureau of Statistics of China, Chinese domestic eggs consumption reached 28,761 kilotons in 2013. Consequently, about 3,164 kilotons of ES (ES account for 11% of the total weight of eggs) were generated, which is a problem because the ES and the attached membrane attract vermin [11]. Despite several literature's findings on the metal ions adsorption on ES [4,12–14], how the ES act on Cd^{2+} in acid aqueous solution remains to be elucidated forward.

On the above summary, the aims of this work are as follows: (1) to understand the removal process of Cd^{2+} in acid aqueous solution by using ES and (2) to seek possible reaction mechanisms from adsorption isotherms, kinetics, surfaces and element analyses.

2. Materials and methods

2.1. ES preparation and characterization

Raw ES were provided by the canteen of the South China University of Technology, Guangzhou, China. The inner shell membranes were manually removed from the ES. Then the ES were washed three times with distilled water to remove impurities before being dried in a muffle furnace at 373 K for 24 h. The materials were ground into granules, and 0.45–1.0 mm sizes were selected using sieves. The obtained ES granules were stored in a desiccator before the experiments.

X-ray fluorescence (XRF-1500, Shimadzu, Japan) was used for the qualitative and quantitative analyses of inorganic compositions of ES. The functional groups of ES surface were identified by Fourier transform infrared (FTIR) spectroscopy (Thermo Fisher Scientific, USA) and prepared ES with KBr discs. The crystallinity of ES was characterized using X-ray diffraction (XRD) (Empyrean, Netherlands) with 2θ angle from 20° to 50°. The external surface morphology and element analyses of ES were examined by scanning electron microscope (SEM; Merlin, Germany) equipped with an energy-dispersive X-ray detector (EDX) for microanalysis.

2.2. Removal procedure

Batch removal experiments were performed using batch reactor systems. The synthetic water with heavy metals was prepared individually by dissolving appropriate amounts of $CdCl_2$, $CuCl_2{\cdot}2H_2O$ and $Pb(NO_3)_2$ in distilled water. All regents were of analytical reagent grade obtained from Sigma-Aldrich Chemical Company (St. Louis, MO, USA).

The effect of Cd^{2+} concentration to solution pH was conducted under different pH parameters (2.5, 3.5, 4.5, 5.5 and 6.5) with different Cd^{2+} concentrations (0, 3.8, 7.6, 15.2, 38, 72, 114 and 152 mg L^{-1}), and 10 g L^{-1} ES in solution at 298 K. The solution with certain initial pH, the changes of pH with increasing Cd^{2+} concentration were recorded by pH analyzer.

Adsorption isotherm experiments were performed at 150 rpm on an orbital shaker with 0.5 g adsorbent in conical flasks containing 50 mL Cd^{2+} solution at different concentrations (about 3.8 to 152 mg L^{-1}) at three temperatures (288, 298 and 308 K). ES and solution were contacted up to 3 d to reach equilibrium (the equilibrium time had been testified by pre-experiment).

Adsorption kinetics experiments were incubated at 150 rpm on an orbital shaker with 10 g ES in conical flasks containing 1 L Cd^{2+} solution (7.6 mg L^{-1}) at three temperatures (288, 298 and 308 K). A fixed volume (5 mL) was withdrawn at designated time points while the reactors were run continuously.

Binary metal competitive study of Cd^{2+}–Cu^{2+} and Cd^{2+}–Pb^{2+} was conducted at 298 K. The dosage of ES was 10 g L^{-1}, and the pH of the solutions was maintained constant of 4.5. Cu^{2+} and Pb^{2+} initial concentrations were the range from 8 to 80 mg L^{-1}, approximately. Cd^{2+} initial concentration was 9.0 mg L^{-1} in solution with Cu^{2+} or Pb^{2+}.

To study ES neutralization to acid aqueous solution, for all experiments (except the experiment of studying the effect of different pH), the pH of cadmium solutions were 4.5 adjusted with HNO_3 or NaOH. These experiments were conducted in duplicate, and all standard errors were within 5%.

2.3. Determination of heavy metals

The concentrations of three heavy metals were determined by a double-beam atomic absorption spectrophotometer, Varian, model SpectrAA-20. The measured concentrations of heavy metals were used to calculate adsorption capacity after equilibrium, q_e (mg g^{-1}), using the following mass balance equation:

$$q_e = \frac{(c_0 - c_e)V}{m} \tag{1}$$

where c_0 and c_e are the initial and equilibrium concentration, mg L^{-1}; V is the initial volume of Cd^{2+} solution, L; m is the mass of ES, g.

3. Results and discussion

3.1. XRF, FTIR and XRD characterizations of raw ES

The results of chemical analysis by XRF indicated that ES had high amount of $CaCO_3$ (97.56%) with less amount of impurities (1.37% $MgCO_3$, 0.45% P_2O_5, 0.44% K_2O and 0.18% others). The phase composition structure of raw ES was also studied further by performing XRD analysis shown in Fig. 1(a). The distinctive peaks (q) were identified as the crystalline phase of calcium carbonate in the calcite form. The crystal structure of calcite was usually described with the trigonal space group [15].

The infrared spectrum of ES is graphed in Fig. 1(b). The strong adsorption peaks at 1,420, 874 and 712 cm^{-1}, and slight peak at 1,790 cm^{-1}, all confirmed the presence of bond C–O, strongly associated with the carbonate minerals, which involved or participated in the binding of heavy metals within ES matrix [16]. The 2,880 and 2,980 cm^{-1} peaks were assigned to bond C–H. The broad band range 3,100–3,500 cm^{-1} attributed to N–H stretching vibration, which is related to the amines and amides of ES membrane [9]. Ho et al. [17] have reported that ES and ES membrane can act as promising 'green' alternatives to remove heavy metals pollutants from wastewater, and there was no difference in the adsorbability of ES and ES with membrane. Therefore, this study will no longer consider the influences of little residual membrane on ES.

3.2. SEM characterization of raw ES and cadmium-laden ES

The SEM images of ES before and after saturated with Cd^{2+} ions (about 150 mg L^{-1}) are displayed in Figs. 2(a) and (b), respectively. To realize the elements in the absorbent, the element mapping of cadmium-laden ES is shown in Fig. 2(c). EDX analyses of ES surfaces in Figs. 2(a) and (b) are performed accordingly, and the resulting spectra are showed in Figs. 2(d) and (e), respectively.

In Fig. 2(a), it can be observed that raw ES had a considerable number of 200–400 nm porosities, which are relatively homogeneous as evidenced by following isotherm studies. Flores-Cano et al. [9] have observed that several crystals with ditrigonal scalenohedral shape and acicular aspect were formed on the surface of ES during Cd^{2+} sorption. The similar crystals are also presented in Figs. 2(b) and (c). Therefore, it can be concluded that the surface precipitation of (Ca, Cd) CO_3 occurred because cadmium ions were incorporated to the trigonal structure of $CaCO_3$ and hexagonal cerussite ($CdCO_3$) formed as well. Xu et al. [18] also indicated that otavite ($CdCO_3$), which yields the lowest lattice misfit with respect to calcite of all metal carbonates, was formed readily as a heteroepitaxial coating on calcite surfaces at ambient conditions. The results in Figs. 2(c) and (e) demonstrated the presence of cadmium element (89.22%) on ES surfaces, thus confirming Cd^{2+} ions precipitation.

3.3. Effect of pH on adsorption capacity

The pH value is a significant controlling parameter to adsorption process. The influence of initial pH (2.5, 3.5, 4.5, 5.5 and 6.5) on ES adsorption capacity to Cd^{2+} is presented in Fig. 3. It can be noted that Cd^{2+} removal has no dramatic enhancement by increasing pH at concentration of 3.8 and 7.6 mg L^{-1}. At 15.2 mg L^{-1}, the amount of Cd^{2+} adsorbed on ES increased at pH of 2.5–4.5 and was almost stable at pH of 4.5–6.5.

It can be explained that H^+ ions competed with Cd^{2+} for the surface sites of adsorbent at lower pH values [19], which would hinder Cd^{2+} ions from reaching the binding sites of sorbent caused by repulsive forces [20]. With the increasing alkalinity, the Cd^{2+} occupied more exchanged sites [21] and got precipitated because of the hydroxide and carbonate anions.

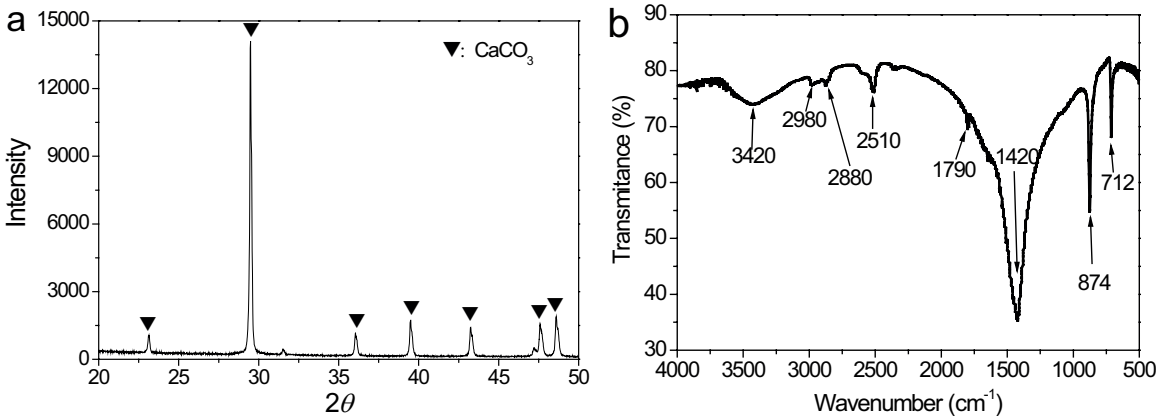

Fig. 1. (a) XRD patterns of raw ES and (b) FTIR spectra of raw ES.

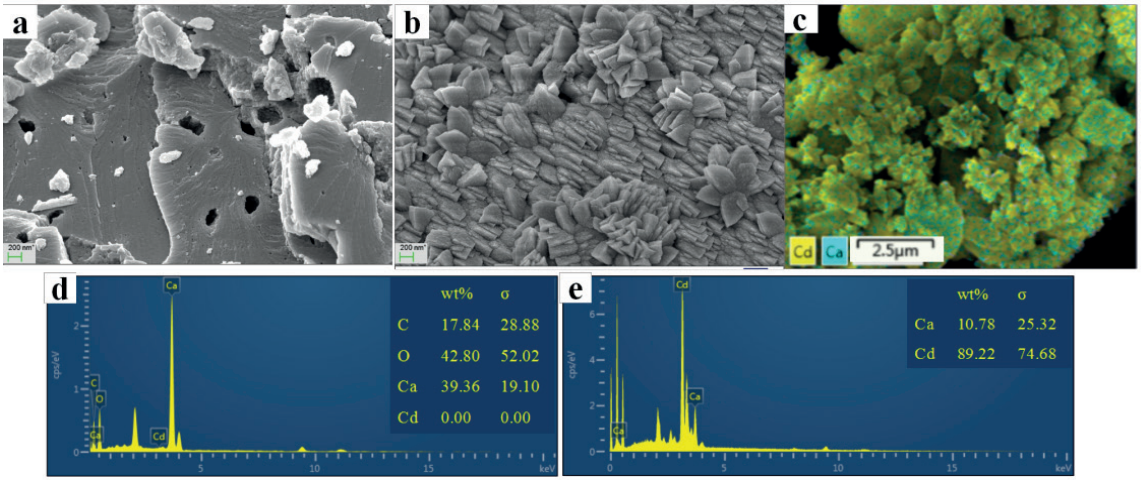

Fig. 2. (a) SEM image of raw ES; (b) SEM image of cadmium-laden ES; (c) element mapping of cadmium-laden ES; (d) EDX spectrum of (a); and (e) EDX spectrum of (b).

3.4. Effect of Cd^{2+} concentration to solution pH

The effect of Cd^{2+} initial concentrations to solution pH is plotted in Fig. 4. After 3 d, without Cd^{2+}, under the influence of 10 g L^{-1} ES, the pH values reached 7.21, 8.09, 9.24, 9.39 and 9.50 in solutions of initial pH of 2.5, 3.5, 4.5, 5.5 and 6.5, respectively. Then the pH values reduced rapidly at beginning stage of Cd^{2+} concentrations increasing, and then they tended to be a steady state. The tendency can be interpreted as follows:

$$CO_3^{2-} + H_2O \rightleftharpoons HCO_3^- + OH^-$$

$$Cd^{2+} + HCO_3^- \rightleftharpoons \equiv CdCO_3 + H^+$$

$$Cd^{2+} + \equiv CaCO_3 \rightleftharpoons \equiv CdCO_3 + Ca^{2+}$$

$$Cd^{2+} + CO_3^{2-} \rightleftharpoons \equiv CdCO_3$$

After adding ES particles to acidic aqueous solution, they dissolved to neutralize acids and increased the concentration of dissolved carbonate. The dissolved calcium carbonate increased the pH of solution above solubility point, which caused metals to precipitate as metal oxide and metal carbonate [22]. Furthermore, based on the lower negative logarithm of solubility product constant, pK_{sp}, of $CaCO_3$ (8.55) than that of $CdCO_3$ (12) [23], the $CdCO_3$ precipitation was more liable to form.

Except precipitation, a small amount of Cd^{2+} was likely retained by ion exchange with Ca^{2+}. Cadmium ions got CO_3^- from HCO_3^- to form $CdCO_3$ and released more H^+ ions as Cd^{2+} concentration increases until no more available carbonate provided. Therefore, the pH of solution decreased as shown in Fig. 4. From the tendency of decreasing pH values, it can be speculated that ion exchange dominated at low concentrations so that more H^+ ions went into the solution, and precipitation dominated at high concentrations for the no more decreases of pH values. Some studies also indicated that both mechanisms involved the characteristic reactions of some metals on $CaCO_3$ surfaces, with cation exchange occurring at low concentrations of metal solution, and precipitation dominating at high concentrations [24].

Therefore, the adsorption experiments should be conducted to calculate the adsorption capacities and analyze the sorption characteristics for the sorption mechanism at low concentration.

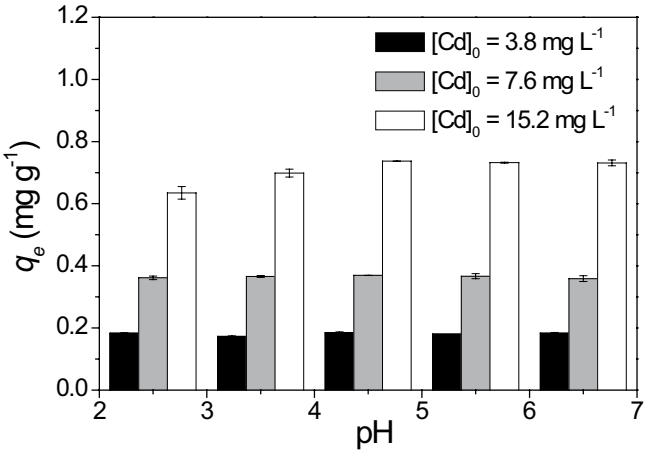

Fig. 3. Adsorption capacity of ES in different pH values at 298 K.

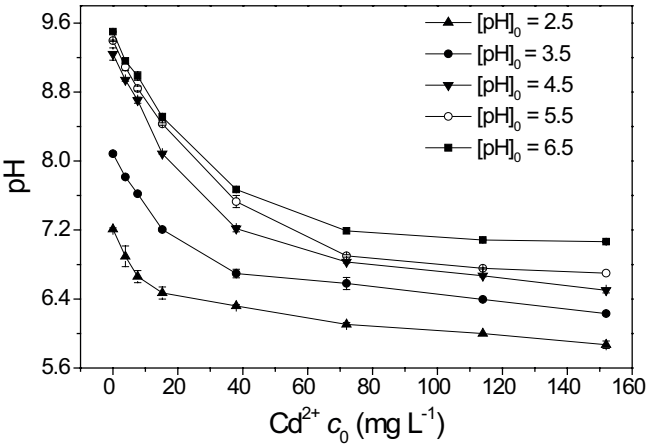

Fig. 4. Effect of initial Cd^{2+} concentrations to solution pH.

3.5. Adsorption isotherms

Langmuir and Freundlich isotherms are applied universally, which describe short-term and monocomponent adsorption of metal ions on different adsorbents [25]. The Langmuir equation is given as follows [26]:

$$q_e = \frac{Q_m b c_e}{1 + b c_e} \tag{2}$$

where q_e and c_e are the equilibrium uptake capacity (mg g^{-1}) and equilibrium concentration (mg L^{-1}), respectively. Q_m is the Langmuir maximum monolayer adsorption capacity (mg g^{-1}), and b is the equilibrium constant. It can be rearranged to a linear form:

$$\frac{c_e}{q_e} = \frac{c_e}{Q_m} + \frac{1}{bQ_m} \tag{3}$$

The Freundlich equation is given as follows [26]:

$$q_e = K_F c_e^{1/n} \tag{4}$$

where K_F and n are Freundlich constants. A linearized form is:

$$\ln q_e = \frac{1}{n} \ln c_e + \ln K_F \tag{5}$$

Linearized isotherms are shown in Fig. 5. Simulated results of Langmuir and Freundlich isotherms are presented in Table 1. The adsorption capacity increased with increasing temperature, which demonstrated that the adsorption process was endothermic. The high correlation coefficients (R^2 > 0.99) showed that Langmuir isotherm fitted adsorption data better than Freundlich isotherm, which indicated that the adsorbent surfaces were homogeneous, and its adsorption

sites included homogeneous capacity [27]. The maximum sorption capacity of ES, Q_m (Table 1), was 2.40 mg g^{-1} at 298 K and increased 1.58 and 1.03 times with temperature increasing from 288 to 298 K and from 298 to 308 K, respectively.

3.6. Adsorption kinetics

Adsorption kinetics is employed to estimate the rate of adsorption process, speculate adsorption mechanism, propose potential rate-controlling step and work out the suitable kinetics model [28]. The pseudo-first-order and pseudo-second-order kinetics models were evaluated for different temperatures in this study.

The pseudo-first-order rate equation is [8,29]:

$$\ln(q_e - q_t) = \ln q_e - k_1 t \tag{6}$$

where q_e and q_t (mg g^{-1}) are the uptake capacity at equilibrium and time t (h), respectively, and k_1 is the rate constant. The k_1 value can be calculated from slopes of linear plots of $\ln(q_e - q_t)$ vs. t.

The pseudo-second-order rate equation is [8,29]:

$$\frac{t}{q_t} = \frac{1}{k_2 q_e^2} + \frac{t}{q_e} \tag{7}$$

where k_2 is the rate constant that can be calculated from slopes of linear plots of t/q_t vs. t. This model is in agreement with chemical sorption being the rate-controlling step [21].

The sorption kinetics in different temperatures is plotted in Fig. 6. The sorption reached equilibrium after 36 h and was divided into two stages: rapid sorption stage (before 10 h) and slow sorption stage (after 10 h). This indicated that Cd^{2+} ions were adsorbed rapidly onto outer surfaces of ES, and then diffused into micropores, which were lying in the interlayer structure of ES. Increasing temperature could enhance the rate of molecular diffusion so that the removal capacity improved for higher temperature.

What's more, Cd^{2+} removal efficiency increased gradually with increasing experimental time and increasing temperature. It reached 87%, 90% and 95% after equilibrium at 288, 298 and 308 K, respectively, as shown in Fig. 6.

Correlative parameters are illustrated in Table 2. The results proved that the pseudo-second-order kinetics better explained the sorption process of Cd^{2+} on ES with high correlation coefficient ($R^2 > 0.999$), and its uptake capacities were more close to the experimental capacities. This showed that the adsorption process was dominated by chemical reaction. From parameters of Table 2, it is also evident that the increasing temperatures favored Cd^{2+} adsorption onto ES.

Using the rate constants, k_2, of pseudo-second-order kinetics model at 288, 298 and 308 K, the activation energy was formulated by linearized Arrhenius equation [21]:

$$\ln k_2 = \ln(A) - (E_a/RT) \tag{8}$$

where E_a is the adsorption activation energy (kJ mol^{-1}); T is the solution temperature (K); A is the Arrhenius constant and R is the ideal gas constant (8.314 J mol^{-1} K^{-1}).

The activation energy is not more than 4.2 kJ mol^{-1} in physical adsorption, owing to its weak force; on the contrary, chemisorption involves force much stronger for activation energy covering a range of 8.4–83.7 kJ mol^{-1} [30]. The activation

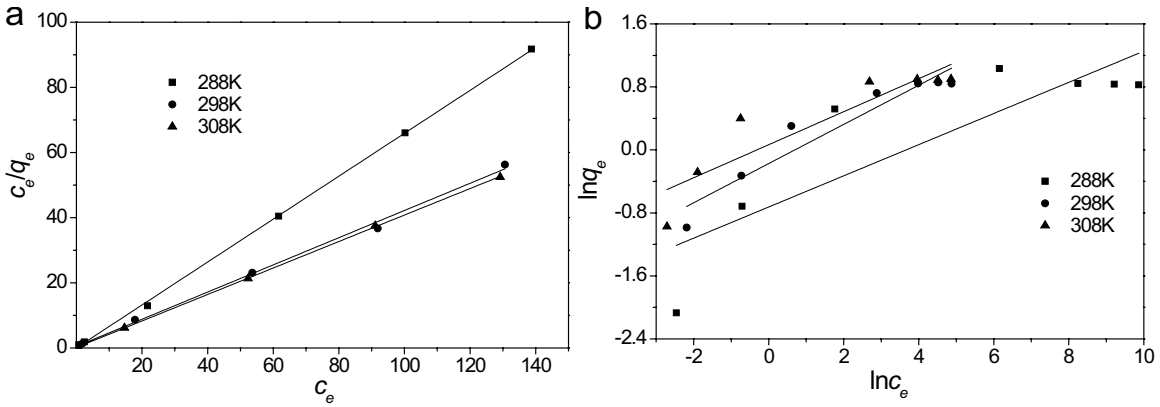

Fig. 5. Linearized isotherms by applying: (a) Langmuir model and (b) Freundlich model.

Table 1
Langmuir and Freundlich models parameters for different temperatures

T (K)	Langmuir model			Freundlich model		
	Q_m (mg g^{-1})	b (L mg^{-1})	R^2	K_F (mg$^{(1-1/n)}$ L$^{1/n}$ g^{-1})	$1/n$	R^2
288	1.5181	0.6587	0.9997	0.4848	0.1979	0.7391
298	2.3964	0.4173	0.9976	0.8407	0.2487	0.9168
308	2.460	0.4065	0.9999	1.068	0.2097	0.8273

energy value of 23.67 kJ mol^{-1} was acquired from the fit of lnk_2 vs. 1/T, which clarified that the system is one of activated chemical adsorption, as was evidenced earlier.

3.7. Thermodynamic parameters

The Gibbs free energy (ΔG), enthalpy (ΔH) and entropy (ΔS) for the adsorption process were obtained using the following formulas [21]:

$$K_d = q_e / c_e \tag{9}$$

$$\ln K_d = \frac{\Delta S}{R} - \frac{\Delta H}{RT} \tag{10}$$

$$\Delta G = \Delta H - T\Delta S \tag{11}$$

$$\Delta G = -RT \ln K_d \tag{12}$$

where T is the temperature, and K_d is the distribution coefficient (mL g^{-1}). The enthalpy change (ΔH) and the entropy (ΔS) can be calculated from a plot of lnK_d vs. 1/T (Fig. 7). The Gibbs free energy was determined at 288, 298 and 308 K. ΔG, ΔH and ΔS were obtained from Eqs. (9)–(12) and given in Table 3.

Values of ΔG indicated the degree of spontaneity of the reaction increased with increasing temperature. Positive value of ΔH indicated the endothermic nature of the process. Positive value of ΔS showed that the affinity of ES for the Cd^{2+} ions.

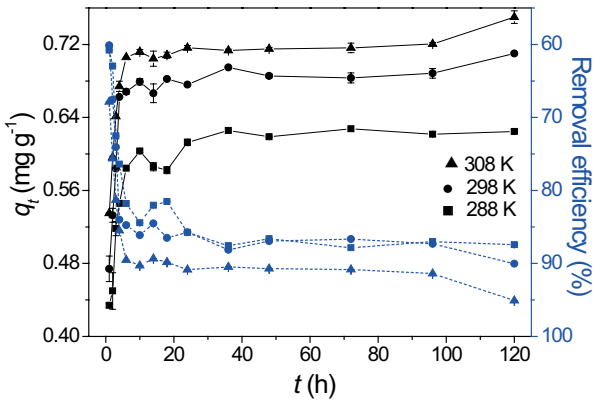

Fig. 6. Sorption kinetics of Cd^{2+} removal capacities (—) and removal efficiencies (- - -) for different temperatures.

3.8. Binary metals competitive experiment

Acid wastewater such as acid mine drainage has different toxic heavy metals including Zn, Mn, Cu, Cd, Pb and As. Especially, Cu^{2+} and Pb^{2+} have higher concentration [31]. To assess the effectiveness of Cd^{2+} uptake on ES in wastewater including other heavy metals, a method combining forward-prediction modeling and laboratory verification was employed, that is studying Cd^{2+}–Cu^{2+} and Cd^{2+}–Pb^{2+} binary metals competitive adsorption.

The plots of binary metals competitive test are given in Fig. 8. On x-axis, Cd^{2+} c_e expresses the Cd^{2+} equilibrium concentrations (mg L^{-1}) after experiment; on y-axis, $[Cu^{2+}]_0/[Pb^{2+}]_0$ signifies the Cu^{2+} or Pb^{2+} initial concentrations. On z-axis, Cd^{2+} q_e denotes the Cd^{2+} equilibrium uptake capacities (mg g^{-1}) in Fig. 8(a); Cu^{2+}/ Pb^{2+} q_e indicates the Cu^{2+} or Pb^{2+} equilibrium uptake capacities (mg g^{-1}) in Fig. 8(b).

In Fig. 8(a), Cd^{2+} sorption capacity on ES decreased with increasing concentrations of Cu^{2+} or Pb^{2+}. And Cu^{2+} shows more obvious inhibitory action to Cd^{2+} sorption especially. With the comparison of curves in Figs. 8(a) and (b), the selectivity order of metal sorption onto ES was found to

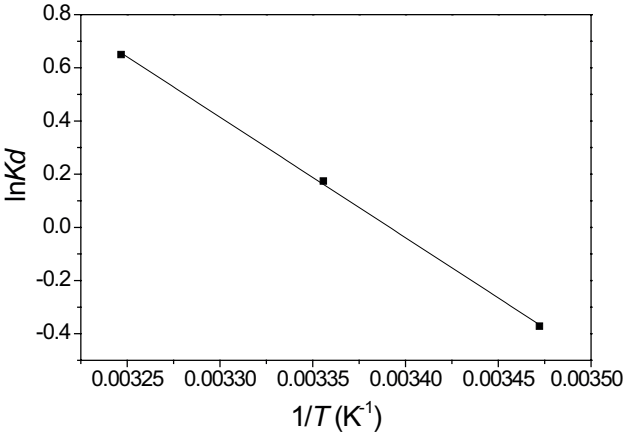

Fig. 7. Plot of lnK_d vs. 1/T.

Table 3
Value of thermodynamic parameters for the adsorption of Cd^{2+} on ES

T (K)	Ea (kJ mol^{-1})	ΔG (kJ mol^{-1})	ΔH (kJ mol^{-1})	ΔS (kJ mol^{-1} K^{-1})
288	23.67	0.010732739	37.679	0.128
298		–0.004855118		
308		–0.017536269		

Table 2
Pseudo-first-order and pseudo-second-order kinetics constants for different temperatures

T (K)	Experimental	Pseudo-first-order model			Pseudo-second-order model		
	q_e (mg g^{-1})	q_e (mg g^{-1})	k_1 (min^{-1})	R^2	q_e (mg g^{-1})	k_2 (g mg^{-1} min^{-1})	R^2
288	0.630	0.1245	0.0376	0.6583	0.628	2.4435	0.9998
298	0.700	0.0798	0.0231	0.4016	0.690	4.2759	0.9999
308	0.721	0.0658	0.0469	0.7255	0.716	4.6211	0.9999

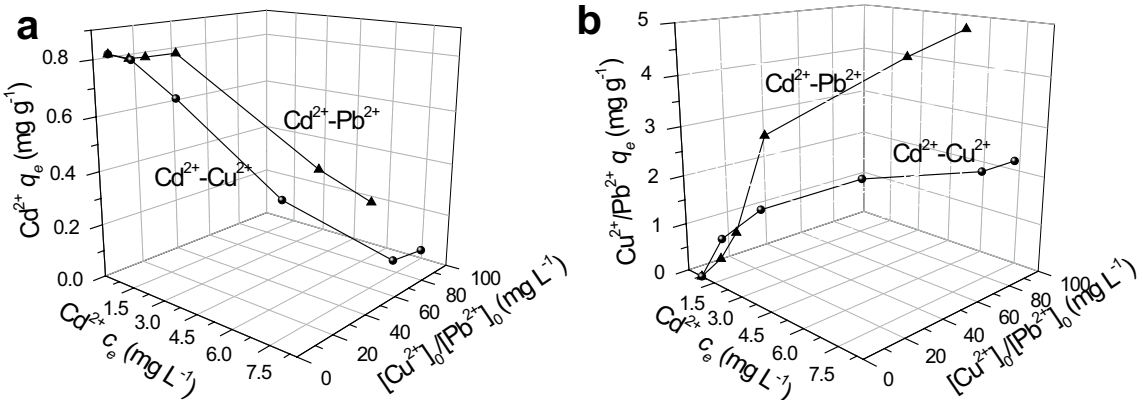

Fig. 8. (a) Effect of Cu^{2+} and Pb^{2+} initial concentrations to Cd^{2+} removal on ES and (b) effect of Cd^{2+} initial concentrations to Cu^{2+} and Pb^{2+} removal on ES.

be: $Cu^{2+} > Cd^{2+} > Pb^{2+}$ at Cu^{2+} and Pb^{2+} concentrations range 8–16 mg L^{-1}, approximately, and $Pb^{2+} > Cu^{2+} > Cd^{2+}$ at their higher concentrations.

It has been illustrated that the heavy metals with smaller radius are more inclined to be adsorbed. Metal ions of lower heat of hydration can fixed in interlayers since they generate interlayer dehydration more easily. The Cu^{2+} has the minimum ionic radius (0.073 nm), and Pb^{2+} has the lowest heat of hydration (1,500.6 kJ mol^{-1}) among three metals [32,33]. Combining the values of pK_{sp} (negative log of the solubility product constants), $CdCO_3$ (12.0) [23], $CuCO_3$ (9.85) [34] and $PbCO_3$ (13.13) [35], it can be speculated that ionic radius played the leading role at low concentrations, and the solubility and heat of hydration dominated advantage at high concentrations. And in solution without or with very low Cu^{2+} and Pb^{2+}, the higher concentration of Cd^{2+} was the driving force for adsorption. Therefore, the competitive sorption will make a difference in the actual acid wastewater.

4. Conclusions

ES, mainly composed of calcium carbonate, were good alkaline adsorbent to remove heavy metals in acid water. The pH values increased rapidly in solution without Cd^{2+}; the increasing rates slowed with increasing Cd^{2+} concentrations, which revealed the main removal mechanisms of precipitation and cation exchange. In binary metal competitive experiment of Cd^{2+}–Cu^{2+} and Cd^{2+}–Pb^{2+}, the selectivity order of metal sorption onto ES was shown to be $Cu^{2+} > Cd^{2+} > Pb^{2+}$ at low Cu^{2+} and Pb^{2+} concentrations and $Pb^{2+} > Cu^{2+} > Cd^{2+}$ at their high concentrations. The Langmuir model fitted the experimental data which certified that the sorption for Cd^{2+} on ES was endothermic and favorable. The pseudo-second-order kinetics and the Arrhenius equation showed the chemical sorption being the rate-controlling step. Cd^{2+} removal efficiency increased with increasing temperature and reached above 90% at 298 K in solution 7.6 mg L Cd^{2+} and 10 g L^{-1} ES. This work indicated that ES has great application potential for removing heavy metals in acid wastewater.

Acknowledgments

The work was financially supported by the National Key Technology Support Program (No. 2015BAD05B05), the Tip-top Scientific and Technical Innovative Youth Talents of Guangdong Special Support Program (No. 2015TQ01Z233), the Science and Technology Program of Guangdong Province (No. 2014A020216004) and the Guangdong Natural Science Funds for Distinguished Young Scholar (No. 2015A030306005).

References

[1] C. Larson, China gets serious about its pollutant-laden soil, Science, 343 (2014) 1415–1416.
[2] Y.S. Ok, J.E. Yang, Y.-S. Zhang, S.-J. Kim, D.-Y. Chung, Heavy metal adsorption by a formulated zeolite – Portland cement mixture, J. Hazard. Mater., 147 (2007) 91–96.
[3] J. Kaduková, E. Virčíková, Comparison of differences between copper bioaccumulation and biosorption, Environ. Int., 31 (2005) 227–232.
[4] P.S. Guru, S. Dash, Sorption on eggshell waste – a review on ultrastructure, biomineralization and other applications, Adv. Colloid Interface Sci., 209 (2014) 49–67.
[5] D. Roy, P.N. Greenlaw, B.S. Shane, Adsorption of heavy metals by green algae and ground rice hulls, J. Environ. Sci. Health., Part A, 28 (1993) 37–50.
[6] S. Lee, Study on the Adsorption Characteristics of Heavy Metals onto the Crab, Portunus trituberculatus shell [D], PhD Thesis, Hyosung Women's University, Daegu, Korea, 1994.
[7] N.V. Farinella, G.D. Matos, M.A. Arruda, Grape bagasse as a potential biosorbent of metals in effluent treatments, Bioresour. Technol., 98 (2007) 1940–1946.
[8] Y. Wang, B.-Y. Gao, W.-W. Yue, Q.-Y. Yue, Adsorption kinetics of nitrate from aqueous solutions onto modified wheat residue, Colloids Surf., A, 308 (2007) 1–5.
[9] J.V. Flores-Cano, R. Leyva-Ramos, J. Mendoza-Barron, R.M. Guerrero-Coronado, A. Aragón-Piña, G.J. Labrada-Delgado, Sorption mechanism of Cd(II) from water solution onto chicken eggshell, Appl. Surf. Sci., 276 (2013) 682–690.
[10] Y.S. Ok, S.-E. Oh, M. Ahmad, S. Hyun, K.-R. Kim, D.H. Moon, S.S. Lee, K.J. Lim, W.-T. Jeon, J.E. Yang, Effects of natural and calcined oyster shells on Cd and Pb immobilization in contaminated soils, Environ. Earth Sci., 61 (2010) 1301–1308.
[11] H.-J. Choi, S.-M. Lee, Heavy metal removal from acid mine drainage by calcined eggshell and microalgae hybrid system, Environ. Sci. Pollut. Res., 22 (2015) 13404–13411.

[12] N. Yeddou, A. Bensmaili, Equilibrium and kinetic modelling of iron adsorption by eggshells in a batch system: effect of temperature, Desalination, 206 (2007) 127–134.
[13] A. Guijarro-Aldaco, V. Hernández-Montoya, A. Bonilla-Petriciolet, M.A. Montes-Morán, D.I. Mendoza-Castillo, Improving the adsorption of heavy metals from water using commercial carbons modified with egg shell wastes, Ind. Eng. Chem. Res., 50 (2011) 9354–9362.
[14] M. Baláž, Z. Bujňáková, P. Baláž, A. Zorkovská, Z. Danková, J. Briančin, Adsorption of cadmium(II) on waste biomaterial, J. Colloid Interface Sci., 454 (2015) 121–133.
[15] R. Przeniosło, P. Fabrykiewicz, I. Sosnowska, Monoclinic deformation of calcite crystals at ambient conditions, Physica B, 496 (2016) 49–56.
[16] D. Beauchemin, J. McLaren, S. Herman, Study of the effects of concomitant elements in inductively coupled plasmamass spectrometry, Spectrochim. Acta, Part B., 42 (1987) 467–490.
[17] J.H. Ho, Y.N. Yeh, H.W. Wang, S.K. Khoo, Y.H. Chen, C.F. Chow, Removal of nickel and silver ions using eggshells with membrane, eggshell membrane, and eggshells, Food Sci. Technol. Res., 20 (2014) 337–343.
[18] M. Xu, L. Kovarik, B.W. Arey, A.R. Felmy, K.M. Rosso, S. Kerisit, Kinetics and mechanisms of cadmium carbonate heteroepitaxial growth at the calcite surface, Geochim. Cosmochim. Acta, 134 (2014) 221–233.
[19] H. Aydın, Y. Bulut, Ç. Yerlikaya, Removal of copper (II) from aqueous solution by adsorption onto low-cost adsorbents, J. Environ. Manage., 87 (2008) 37–45.
[20] E. Malkoc, Y. Nuhoglu, Removal of Ni(II) ions from aqueous solutions using waste of tea factory: adsorption on a fixed-bed column, J. Hazard. Mater., 135 (2006) 328–336.
[21] L. Zheng, Z. Dang, X. Yi, H. Zhang, Equilibrium and kinetic studies of adsorption of Cd(II) from aqueous solution using modified corn stalk, J. Hazard. Mater., 176 (2010) 650–656.
[22] H.A. Aziz, M.N. Adlan, K.S. Ariffin, Heavy metals (Cd, Pb, Zn, Ni, Cu and Cr(III)) removal from water in Malaysia: post treatment by high quality limestone, Bioresour. Technol., 99 (2008) 1578–1583.
[23] S.K. Thakur, N.K. Tomar, S.B. Pandeya, Influence of phosphate on cadmium sorption by calcium carbonate, Geoderma, 130 (2006) 240–249.
[24] M.B. Mcbride, Chemisorption and precipitation of Mn^{2+} at $CaCO_3$ surfaces, Soil. Sci. Soc. Am. J., 43 (1979) 693–698.
[25] D. Sud, G. Mahajan, M. Kaur, Agricultural waste material as potential adsorbent for sequestering heavy metal ions from aqueous solutions–a review, Bioresour. Technol., 99 (2008) 6017–6027.
[26] M.R. Sangi, A. Shahmoradi, J. Zolgharnein, G.H. Azimi, M. Ghorbandoost, Removal and recovery of heavy metals from aqueous solution using *Ulmus carpinifolia* and *Fraxinus excelsior* tree leaves, J. Hazard. Mater., 155 (2008) 513–522.
[27] S. Gupta, B.V. Babu, Utilization of waste product (tamarind seeds) for the removal of Cr(VI) from aqueous solutions: equilibrium, kinetics, and regeneration studies, J. Environ. Manage., 90 (2009) 3013–3022.
[28] A.Y. Dursun, C.S. Kalayci, Equilibrium, kinetic and thermodynamic studies on the adsorption of phenol onto chitin, J. Hazard. Mater., 123 (2005) 151–157.
[29] X. Yang, B. Al-Duri, Kinetic modeling of liquid-phase adsorption of reactive dyes on activated carbon, J. Colloid Interface Sci., 287 (2005) 25–34.
[30] Z. Aksu, G. Karabayır, Comparison of biosorption properties of different kinds of fungi for the removal of Gryfalan Black RL metal-complex dye, Bioresour. Technol., 99 (2008) 7730–7741.
[31] M. Chen, G. Lu, C. Guo, C. Yang, J. Wu, W. Huang, N. Yee, Z. Dang, Sulfate migration in a river affected by acid mine drainage from the Dabaoshan mining area, South China, Chemosphere, 119 (2015) 734–743.
[32] D.A. Sverjensky, N. Sahai, Theoretical prediction of single-site surface-protonation equilibrium constants for oxides and silicates in water, Geochim. Cosmochim. Acta, 60 (1996) 3773–3797.
[33] N. Sahai, D.A. Sverjensky, Solvation and electrostatic model for specific electrolyte adsorption, Geochim. Cosmochim. Acta, 61 (1997) 2827–2848.
[34] J.M. Sun, X.H. Zhao, J.C. Huang, Characterization of adsorbent composition in co-removal of hexavalent chromium with copper precipitation, Chemosphere, 58 (2005) 1003–1010.
[35] C.-S. Chen, Y.-J. Shih, Y.-H. Huang, Remediation of lead (Pb(II)) wastewater through recovery of lead carbonate in a fluidized-bed homogeneous crystallization (FBHC) system, Chem. Eng. J., 279 (2015) 120–128.